

“Weather” art thy climate? Climate representativeness in rigid pavement design

Anushka Khachi¹ and Sushobhan Sen^{*2}

¹Department of Civil Engineering, Indian Institute of Technology Gandhinagar, Palaj, Gandhinagar, Gujarat-382355, India, E-mail: anushka.khachi@iitgn.ac.in

²Department of Civil Engineering, Indian Institute of Technology Gandhinagar, Palaj, Gandhinagar, Gujarat-382355, India, E-mail: sushobhan.sen@iitgn.ac.in

Abstract

Climatic conditions significantly influence the performance of Jointed Plain Concrete Pavements (JPCPs). Variations in temperature, wind speed, solar radiation and other factors generate non-linear temperature distributions. These distributions result in curling stresses and eigenstresses that increase the fatigue damage and thus reduce the expected service life of the section. Mechanistic-Empirical JPCP design relies on historical weather data of several years to generate temperature profiles for performance prediction. However, determining the optimal duration of historical data needed for reliable predictions remains unknown. Limited datasets may overlook long-term trends and variability, while an overly extensive dataset may increase computational time without significantly improving accuracy. This study aims to investigate the climatological representativeness of various weather data sources for assessing JPCP performance. Weather data spanning 30 years, which is the accepted definition of climate representativeness, was examined in comparison with 15 years of data and a statistical dataset called a Typical Meteorological Year (TMY) for both periods. These datasets were used to numerically evaluate the temperature profiles through various JPCP sections, and the performance of those sections was assessed based on curling and eigenstresses developed. In particular, the thickness and the solar reflectance (albedo) of the JPCP sections were varied to understand the extent to which climate representativeness depends on these properties. The analysis revealed that the distributions of temperature differences and eigenstresses for 15 years, 30 years and their respective TMYs align closely. However, the 30 years of data consists of more extremes than 15 years period. The TMYs for both 30 years and 15 years period show similar results. Hence, for design, if the extreme events are not considered, then 15 years' TMY can be used. However, if extremes are to be considered, then 30 years of historical should be considered.

1 Introduction

The climatic conditions of an area, in addition to the vehicular loading, leads to the development of stresses within Jointed Plain Concrete Pavements (JPCPs). The interaction between a JPCP section and its surrounding environment leads to the generation of non-linear temperature distributions within the concrete slab, which have been extensively studied over in the past [1–4]. These non-linear temperature gradients significantly influence pavement performance, particularly when combined with vehicular loading. Daily and seasonal temperature fluctuations cause the pavement slab to undergo curling, driven

*Corresponding Author

by the difference expansion and contraction of the top and bottom surfaces. During the daytime, the surface of the slab typically absorbs solar radiation and becomes warmer than the bottom, resulting in a positive temperature difference (ΔT) that leads to upward curling. When subjected to vehicular loading, this contributes to bottom-up cracking. Conversely, at night, the slab surface cools down faster than the bottom, creating a negative temperature difference. This reversal in the temperature profile induces downward curling which, under vehicular loading at critical positions, leads to top-down cracking.

In 1940, Thomlinson [5] developed a theory to evaluate the influence of non-linear temperature distributions on JPCP sections. He proposed decomposing the non-linear temperature profile into three components: (a) a constant component T_C , representing a uniform temperature change that causes uniform expansion or contraction, (b) a linear temperature component $T_L(z)$, which generates curling stresses due to restrictions to curling imposed by the slab's self-weight, subgrade, and vehicular load, and (c) a non-linear component $T_N(z)$, which produces self-equilibrating eigenstresses within the pavement structure [2]. While the linear component is commonly considered in pavement design, there is a growing recognition of the importance of eigenstresses (σ_N). As noted by Choubane and Tia (1992)[2], current codes for concrete pavements predominantly focus on the linear components of the temperature distribution, neglecting the nonlinear aspects, which can lead to significant underestimation of total thermal stresses [6–8]. These curling stresses and eigenstresses, resulting from non-linear temperature distributions, contribute to the total stresses within the pavement. Therefore, a comprehensive understanding of both the linear and nonlinear components of temperature-induced stresses is crucial for enhancing the longevity and performance of rigid pavements, particularly in regions with significant temperature variations.

The design of Jointed Plain Concrete Pavements (JPCP) using the Mechanistic-Empirical Pavement Design Guide (MEPDG) in the US [9, 10] relies on accurately modelling pavement temperature profiles using the Enhanced Integrated Climatic Model (EICM)[11]. This model simulates temperature distributions based on historical hourly weather data for the design period. Other countries have also adopted design standards that are based on the MEPDG, where such data is also required. Given a service life of 30 or more years, this amounts to over 250,000 hours of weather data that need to be analyzed for every trial section in the design process, which is a huge computational burden. An alternative approach is to perform the temperature analysis for fewer years but such that the results are representative of the rest of the service life. A key challenge in this process is determining the optimal duration of historical weather data necessary for reliable predictions. While short-term datasets may not adequately capture long-term climate variability, seasonal extremes, and trends, excessively long datasets can lead to increased computational time without significantly enhancing prediction accuracy.

One such representative weather dataset is the Typical Meteorological Year (TMY). A TMY is essentially a yearly dataset that is climatologically representative of the long-term weather data at a particular location. The months in a TMY are selected from corresponding months across multiple years within the designated period, and so TMY is not a synthetically-generated dataset but rather consists of past weather data. In 1978, Hall et al. [12] developed a method for TMY generation, which has since evolved into various forms, including test reference year (TRY), typical meteorological year(TMY), TMY2 [13], TMY3, weather year for energy calculations (WYEC) [14], WYEC2 [15]. The most common application of these datasets is in building energy simulations[16–18].

This study aims to investigate the climatological representativeness of various weather data sources in assessing the performance of JPCP sections. Weather data spanning 30 years, which is the accepted standard for climate representativeness, was examined alongside 15 years of data and a statistical dataset known as a Typical Meteorological Year (TMY). The analysis was conducted for the city of Ahmedabad in Gujarat, India, covering the periods from 1992 to 2021 (30 years) and from 2007 to 2021 (15 years, the most recent ones). TMYs were generated for both time frames. For this study, TMYs were produced using the TMY3 User Manual(National Renewable Energy Laboratory's latest TMY collection) [19] for both time periods. Additionally, a one-dimensional Finite Element Method-based model was developed to generate the hourly temperature profile throughout the JPCP slab section. The comparison among the different data sources was

made based on the linear temperature differences and eigenstresses generated. Moreover, the thickness and the solar reflectance (albedo) of the JPCP sections were also varied to understand the extent to which climate representativeness depends on JPCP properties. Finally, statistical analysis was performed to compare the 30 years of weather data with the 15 years and their corresponding TMYs to determine the length of weather data sufficient to represent climate conditions in JPCP design. This analysis helps optimise the computational effort required for precise JPCP section design based on mechanistic-empirical principles.

2 Methodology

This study compares historical climate data spanning 30 years (1992–2021) and 15 years (2007–2021) with their corresponding TMYs based on two key analysis parameters: linear temperature difference (ΔT) and critical eigenstresses (σ_N) in JPCP sections. The analysis considers slab thicknesses of 150 mm, 200 mm, 250 mm, and 300 mm, as well as two albedo values for the PCC slab: 0.3 and 0.5. The location is assumed to be Ahmedabad, a city in Gujarat, India, but the approach can be used anywhere else as well.

2.1 Weather Data

For Ahmedabad, this study utilizes the latest ERA5 climate reanalysis data from the European Centre for Medium-Range Weather Forecasts (ECMWF) [20]. ERA5 provides hourly data on various atmospheric, land surface, and sea state parameters going back to 1960. The present analysis considers historical hourly data for two periods: 1992–2021 (30 years) and 2007–2021 (15 years). Thirty years of weather data is the most widely accepted definition of "climate". The ERA5 dataset is structured on a grid with a $0.25^\circ \times 0.25^\circ$ resolution. Since Ahmedabad's exact location is not exactly at a reanalysis grid point, bilinear interpolation was used to spatially downscale the data.

The TMY data for the two time periods were produced using the TMY3 User Manual [19]. The short-term monthly cumulative distribution functions (CDFs) (calculated for all years under consideration) corresponding to nine daily indices (mean, maximum, and minimum dry bulb and dew point temperatures, the mean and maximum wind velocity, and the total global horizontal solar radiation) were compared with the long-term CDF for each month. Then, five candidate months closest to the long-term CDF were ranked in the increasing order of WS statistic, where WS statistic is a weighted sum of the Finkelstein- Schafer (FS) statistics, which compares candidate monthly CDF with long-term CDF. The FS statistics is given by Eq. 1.

$$FS = \left(\frac{1}{n}\right) \sum_{i=1}^n \delta_i \quad (1)$$

Where ,

δ_i = Absolute difference between the long-term CDF and the candidate month CDF for any index

n = Number of daily readings in a month.

And the WS statistic is given by Eq. 2, where w_i = weight of the index i (defined in [19]) and FS_i = FS statistic for index i .

$$WS = \sum w_i FS_i \quad (2)$$

For the five candidate months, persistence criteria defined by Hall [12] were used to select among the five candidate months the Typical Meteorological Month. The persistence criterion excludes candidate months with extreme values from consideration. The persistence of mean dry bulb temperature and daily global horizontal radiation is assessed by analyzing the frequency and run lengths exceeding or falling below fixed long-term percentiles. Here, run length is defined as the number of consecutive days (two or more) in a month that are either above or below the long-term percentiles. These are determined

by sorting the values of the specific parameter in ascending order. Frequency refers to the total number of such runs for a given month. For mean daily dry bulb temperature, the frequency and run length above the 67th percentile and below the 33rd percentile are evaluated. For global horizontal radiation, only the frequency and run lengths below the 33rd percentile are considered. According to the persistence criterion, the months with the longest run, the most runs, and the month with no runs are disqualified. The highest-ranked candidate month, based on WS values in ascending order and meeting the persistence criterion, is selected for the TMY. The 12 chosen months are then combined to form a complete year, with curve-fitting techniques applied to smooth discontinuities at monthly transitions over a six-hour period on either side.

2.2 Temperature Profile Generation and Decomposition

The historical climate data from 1992-2021 and 2007-2021, along with corresponding TMY datasets, were used to generate hourly temperature distributions T within the pavement layers. This was done using the previously-developed 1D thermal model, ILLI-THERM [21]. The model discretises the pavement depth into nodes, each assigned specific thermal properties such as conductivity k , density ρ , and heat capacity c_p , based on the layer composition. Reasonable assumptions were made for all layer properties. A one-dimensional heat equation, as given in Equation 3 (where t is time and z is the depth through the JPCP section), was solved using the backward Euler scheme to ensure numerical stability. The initial condition was assumed to be uniform throughout the pavement depth equal to the air temperature. The surface boundary condition was formulated using an energy balance equation that accounted for solar radiation, convection, and radiation losses, while the bottom boundary was treated as an adiabatic. The model considered varying slab thicknesses (150, 200, 250, and 300 mm) and albedo values (0.3 and 0.5) to evaluate their influence on pavement temperature.

$$\rho c_p \frac{\partial T}{\partial t} = \frac{\partial}{\partial z} \left(k \frac{\partial T}{\partial z} \right) \quad (3)$$

The hourly temperature profiles generated using the numerical model were further decomposed into the constant T_C , linear $T_L(z)$ and non-linear components $T_N(z)$ considering the concrete slab as homogeneous and isotropic [22] using Equations 4 - 6. The integrals were evaluated numerically using the Trapezoidal rule, with reference temperature $T_0 = 0^\circ\text{C}$.

$$T_c(z) = \frac{1}{h} \int_{-h/2}^{h/2} T(z) dz \quad (4)$$

$$T_L(z) = T_0 + \frac{12z}{h^3} \int_{-h/2}^{h/2} T(z) z dz \quad (5)$$

$$T_N = T_0 + T(z) - \frac{1}{h} \int_{-h/2}^{h/2} T(z) dz - \frac{12z}{h^3} \int_{-h/2}^{h/2} T(z) z dz \quad (6)$$

The eigenstress distribution within the slab was calculated using Equation 7.

$$\sigma_N(z) = -\frac{E\alpha}{1-\nu} (T_N(z) - T_0) \quad (7)$$

Where E = Young's modulus (assumed to be 30 GPa), α = coefficient of thermal expansion (assumed to be $10^{-5}/^\circ\text{C}$), and ν = Poisson's ratio (assumed to be 0.30).

The design of JPCPs primarily considers the linear component of temperature distribution T_L . Using this component, the temperature difference between the top and bottom of the concrete layer, denoted as ΔT , was determined. During the daytime, a positive ΔT leads to bottom-up cracking, whereas at night, a negative ΔT results in top-down cracking. Additionally, Critical Eigenstress Ratio (CESR) was computed at

the critical locations for both top-down and bottom-up cracking scenarios to account for the influence of eigenstresses on total stresses. CESR represents the ratio of the critical eigenstress associated with a specific failure mode to the slab's flexural strength, which was assumed to be 4.5 MPa in this study. The CESR was evaluated at the top of the slab for top-down cracking and at the bottom for bottom-up cracking.

3 Results and discussion

The hourly temperature profiles generated using the numerical analysis for the 2007-2021 and 1992-2021 time periods with their corresponding TMYs were decomposed, and the linear temperature differences and eigenstresses were calculated for both top-down and bottom-up cracking cases. The comparison between the 15-year and 30-year historical datasets with their corresponding TMYs for temperature difference distribution is shown in Figure 1(a) and (b) for albedos of 0.3 and 0.5, respectively, for top-down cracking.

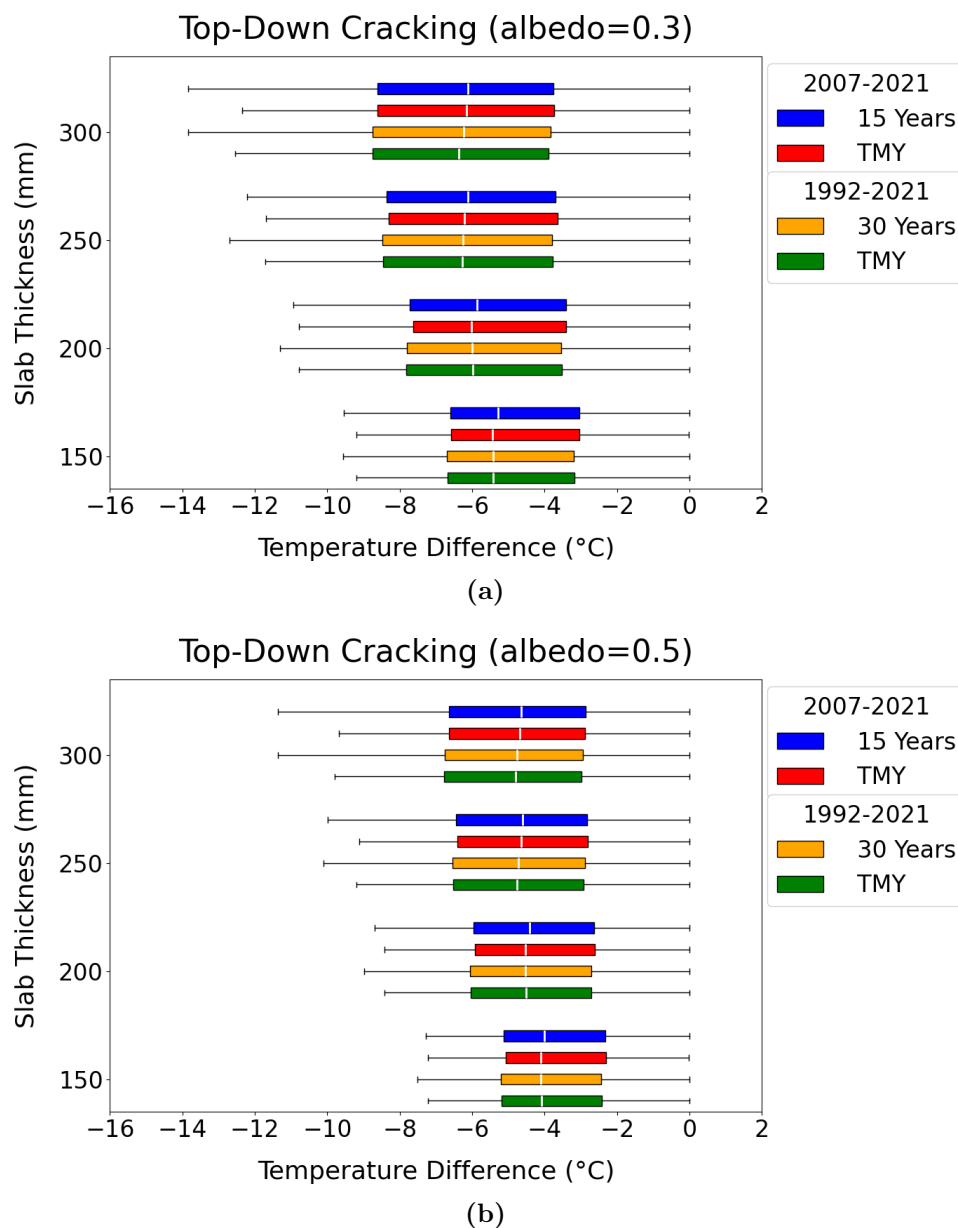
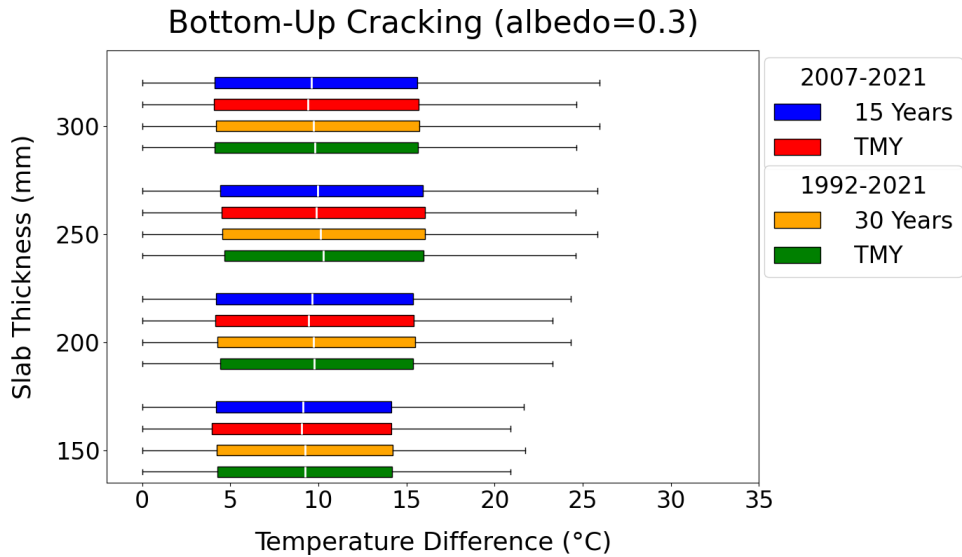


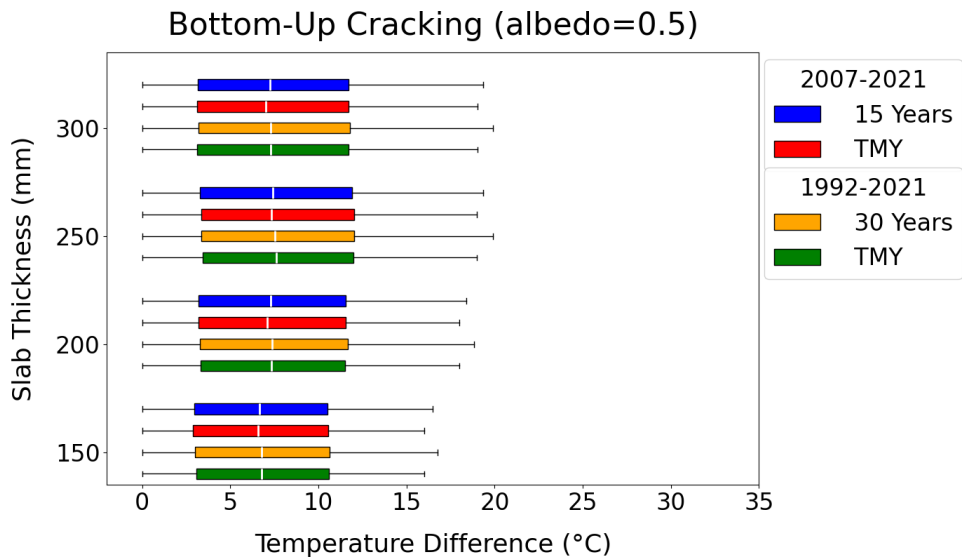
Figure 1: Statistical comparison between 15 years data, 30 years data, and corresponding TMYs for (a) albedo of 0.3 and (b) albedo of 0.5 based on linear temperature differences for Top-Down cracking

A clear increase in the temperature difference values is observed with increasing slab thickness, which is attributed to the higher thermal inertia of thicker slabs leading to larger temperature gradients. Pavement surfaces with a lower albedo of 0.3 consistently exhibit higher temperature differences compared to those with an albedo of 0.5, highlighting the role of solar reflectance, where lower albedo results in greater solar absorption and higher surface temperatures. Across different weather datasets, the median temperature difference values align closely with each other, with only minor differences between the 15- and 30-year datasets as well as their corresponding TMYs. However, more extreme values are observed in the actual historical datasets (15-year and 30-year datasets) as compared to the TMY datasets. This is a direct consequence of the persistence criteria used in generating TMYs, excluding extreme events by removing months above or below specific thresholds from the candidate months list. The TMYs across both time periods show similar trends, while the 30-year historical data consists of more extreme values than the 15-year actual dataset.

The TMY datasets, while having similar medians as their full 15- or 30-year counterparts, show less variability. This reduced variability may facilitate better predictability in design but could underestimate risks from extreme climate conditions. The higher temperature differences in thicker pavements and lower albedo cases imply a higher susceptibility to cracking, emphasising the need for careful consideration of slab thickness and surface albedo in pavement design. Furthermore, pavements with higher albedo (i.e., 0.5) demonstrate reduced temperature differences, which not only mitigate thermal cracking but also contribute to improved sustainability. This observation agrees with that reported in earlier literature as well [23]. Similar observations can be seen in the bottom-up cracking case for the temperature differences, as shown in Figure 2.



(a)



(b)

Figure 2: Statistical comparison between 15 years data, 30 years data, and corresponding TMYs for (a) albedo of 0.3 and (b) albedo of 0.5 based on linear temperature differences for Bottom-up cracking

The comparison for the Critical Eigenstress Ratio (CESR) for the top-down cracking case is presented in Figure 3(a) and (b) for albedo values of 0.3 and 0.5, respectively. Across all slab thicknesses, the median CESR values are consistently positive, indicating that the pavement layers are predominantly in a state of tensile eigenstress, which is a critical factor contributing to total pavement stresses. The tensile nature of the CESR highlights the potential vulnerability of the pavement to cracking, especially under repeated thermal and traffic loading.

The comparison between the 15-year and 30-year historical datasets and their respective TMYs reveals a similar trend as observed in the temperature difference analysis. The TMY datasets exhibit distributions with fewer extreme values, indicating a smoothing of extreme stress values. In contrast, the historical datasets, particularly the 30-year data, show a broader range of CESR values and more extreme values, reflecting the inherent variability and extreme conditions present in actual weather data.

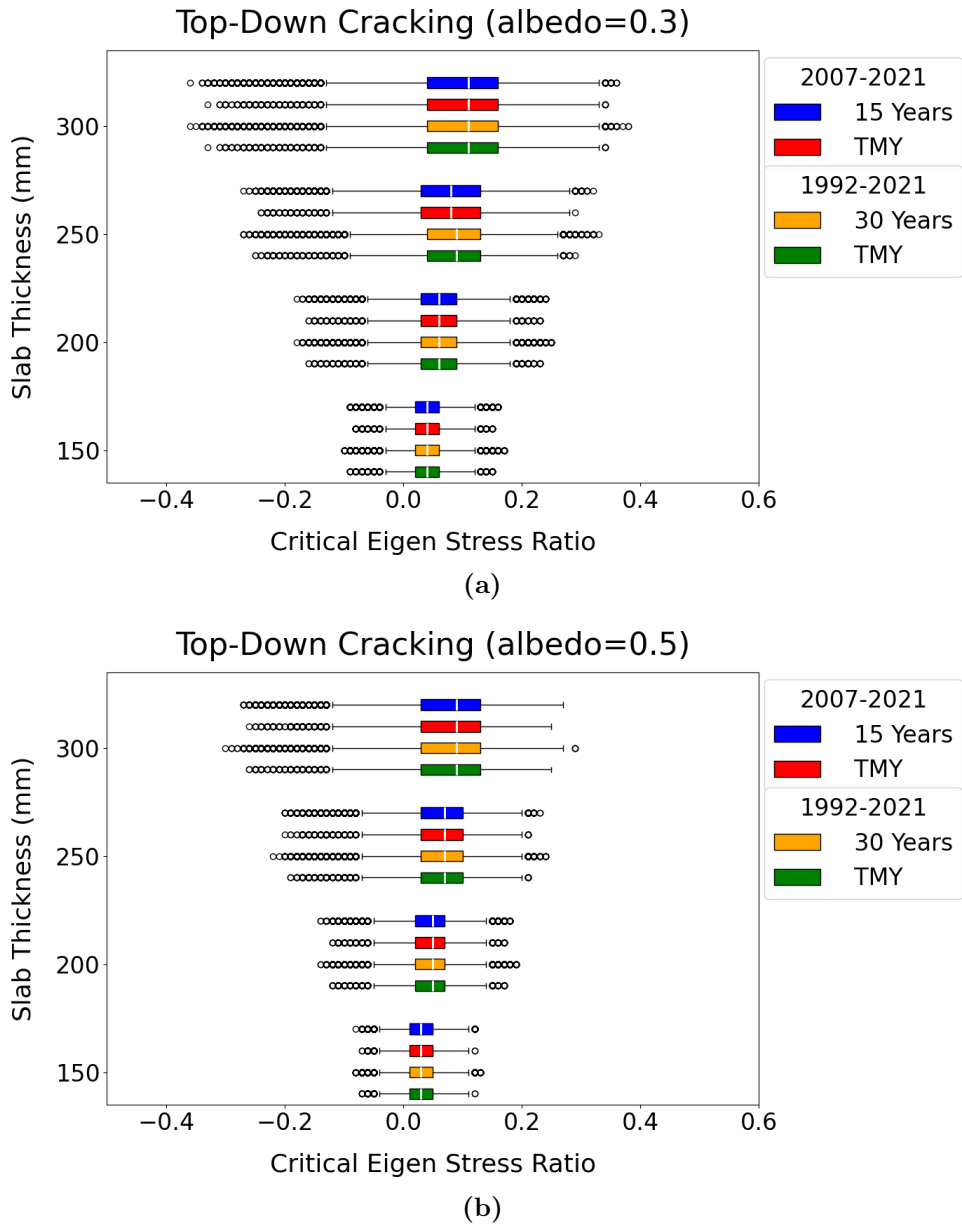
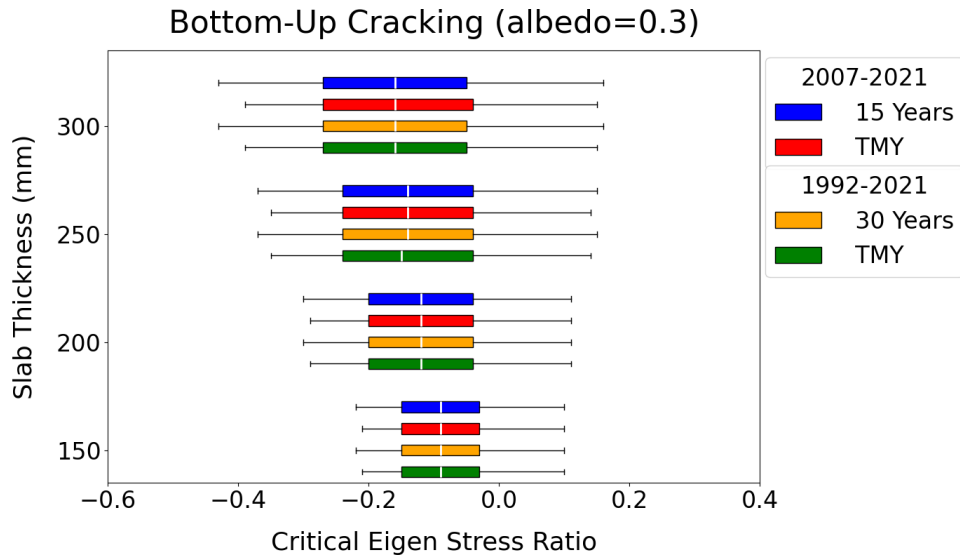
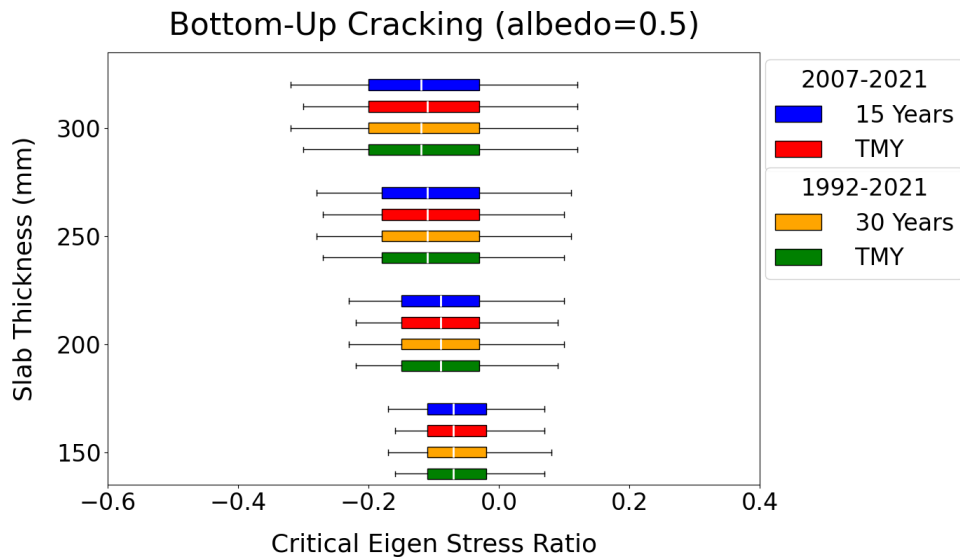


Figure 3: Statistical comparison between 15 years, 30 years data, and corresponding TMYs for (a) albedo of 0.3 and (b) albedo of 0.5 based on CESR for Top-Down cracking

Furthermore, the influence of albedo is clearly visible from the data. JPCP sections with an albedo of 0.3 exhibit higher CESR values as compared to those with an albedo of 0.5. The reduced CESR values in pavements with higher albedo highlight the mitigating effect of increased solar reflectance, which not only reduces tensile stresses but also contributes to overall pavement performance. These findings emphasize the importance of considering both slab thickness and surface albedo in pavement design to mitigate the risk of top-down cracking effectively. Similarly, Figure 4 shows the CESR distribution for the Bottom-up cracking case, where the median CESR values across all slab thicknesses and albedo are negative, indicating compressive eigenstresses. For the bottom-up cracking case, fewer extreme values can be seen as compared to the top-down cracking case; however, the observations are similar. In particular, it can be observed that although the median values are negative, the distributions also include several positive values (i.e., tensile eigenstresses) as well, especially with increasing slab thickness. This phenomenon of higher eigenstresses for thicker slabs has been reported in earlier literature as well [24].



(a)



(b)

Figure 4: Statistical comparison between 15 years, 30 years data, and corresponding TMYs for (a) albedo of 0.3 and (b) albedo of 0.5 based on CESR for Bottom-up cracking

Finally, a two-way ANOVA test was conducted to examine the impact of different datasets and time periods on temperature differences and CESR values. The results indicated that the dataset (whether it was TMY data or the full reanalysis data) did not have a significant effect on either parameter at a significance level of 0.05. This suggests that both data types yield comparable results for these parameters. However, the analysis period (15 years versus 30 years) has a significant effect on both parameters, highlighting the importance of considering longer time frames for a more comprehensive assessment of temperature variations and CESR values. These findings emphasise that while the choice of data type may not be critical, the duration of the analysis plays a crucial role in capturing long-term trends. Moreover, if the designer wishes to incorporate the effects of extreme climatic events, the full 30-year analysis would be preferable despite its higher computational demand.

4 Conclusion

Jointed Plain Concrete Pavements (JPCPs) are exposed to climatic variations over their service life, including changes in temperature, wind speed, and solar radiation, which significantly affect their long-term performance. These variations create non-linear temperature profiles within the pavement, leading to stresses that affect their performance. Mechanistic-empirical pavement design for JPCPs relies on accurately characterising these temperature profiles, typically using extensive historical weather datasets over the entire service life of the section. However, the optimal amount of historical weather data required for reliable performance predictions is still unclear. While longer datasets may provide a more comprehensive view of climatic variability, they also increase computational effort. Conversely, shorter datasets might overlook critical trends and extreme events, which could compromise the reliability of the design.

To address this issue, this study analyzed the climatological representativeness of various weather data sources for evaluating JPCP performance. Specifically, the temperature differential and the resulting eigenstresses were assessed using 30 years of historical weather data, 15 years of historical data, and Typical Meteorological Year (TMY) datasets derived from both periods, with the city of Ahmedabad, India as an illustrative case. The analysis also included variations in pavement thickness (i.e. 150, 200, 250 and 300 mm) and surface albedo (0.3 and 0.5) to explore the influence of structural and material properties on temperature-induced stresses.

The study highlights that slab thickness, albedo, and climate variability play a crucial role in influencing temperature differences and critical eigenstress ratios (CESR) in JPCP slabs. Thicker slabs exhibit higher thermal gradients and CESR values, increasing the risk of cracking, while higher albedo surfaces effectively reduce thermal gradients and tensile stresses, demonstrating the importance of solar reflectance in mitigating surface cracking. Additionally, it was observed that TMY data for both 15-year and 30-year periods exhibit similar median values for temperature differences and CESR values, indicating that the time frame of the TMY does not significantly impact the results. However, reanalysis data reveals more extreme values, especially in the 30-year period, reflecting the impact of extreme climatic events. Thus, while TMY data can suffice for general analyses, historical data is essential for capturing extreme events, where the time frame of analysis also becomes critical. However, this study is limited to one location, and the observations may vary with regional climatic conditions. Future studies should expand the analysis to multiple locations and time periods to better understand the interplay between climate and pavement performance, enabling the design of more resilient pavement systems.

5 Acknowledgments

This study was enabled by a fellowship received by Anushka Khachi from IIT Gandhinagar.

References

- [1] J. M. Armaghani, T. J. Larsen, and L. L. Smith, *Temperature response of concrete pavements*. No. 1121, 1987.
- [2] B. Choubane and M. Tia, “Nonlinear temperature gradient effect on maximum warping stresses in rigid pavements,” *Transportation Research Record*, vol. 1370, no. 1, p. 11, 1992.
- [3] J.-H. Jeong and D. G. Zollinger, “Environmental effects on the behavior of jointed plain concrete pavements,” *Journal of Transportation Engineering*, vol. 131, no. 2, pp. 140–148, 2005.
- [4] S. Sen and L. Khazanovich, “Reconsidering the strength of concrete pavements,” *International Journal of Pavement Engineering*, vol. 24, no. 2, p. 2020270, 2023.

- [5] J. Thomlinson, “Temperature variations and consequent stresses produced by daily and seasonal temperature cycles in concrete slabs,” *Concrete Constructional Engineering*, vol. 36, no. 6, pp. 298–307, 1940.
- [6] S. Schmid, R. D. Flores, M. Aminbaghai, B. Pichler, L. Eberhardsteiner, R. Blab, and H. Wang, “Curling stresses and thermal eigenstresses in a concrete pavement slab,” in *Computational Modelling of Concrete and Concrete Structures*, pp. 564–571, CRC Press, 2022.
- [7] S. J. Schmid, R. Díaz Flores, M. Aminbaghai, L. Eberhardsteiner, H. Wang, R. Blab, and B. L. Pichler, “Significance of eigenstresses and curling stresses for total thermal stresses in a concrete slab, as a function of subgrade stiffness,” *International Journal of Pavement Engineering*, vol. 24, no. 2, p. 2091136, 2023.
- [8] B. Choubane and M. Tia, “Analysis and verification of thermal-gradient effects on concrete pavement,” *Journal of Transportation Engineering*, vol. 121, no. 1, pp. 75–81, 1995.
- [9] O. NEW and R. PAVEMENT, “Guide for mechanistic-empirical design,” *Washington DC*, 2004.
- [10] Q. Li, D. X. Xiao, K. C. Wang, K. D. Hall, and Y. Qiu, “Mechanistic-empirical pavement design guide (mepdg): a bird’s-eye view,” *Journal of Modern Transportation*, vol. 19, pp. 114–133, 2011.
- [11] M. W. W. C. E. Zapata, D. Andrei and W. N. Houston, “Incorporation of environmental effects in pavement design,” *Road Materials and Pavement Design*, vol. 8, no. 4, pp. 667–693, 2007.
- [12] I. J. Hall, P. RR, A. HE, and B. EC, “Generation of typical meteorological years for 26 solmet stations,” 1979.
- [13] “User’s manual for tmy2s - typical meteorological years,” 6 1995.
- [14] L. W. Crow, “Weather year for energy calculations,” *ASHRAE J.:(United States)*, vol. 26, 1984.
- [15] J. R. Augustyn, “Wyec2 user’s manual and software toolkit,” *ASHRAE Transactions*, vol. 104, p. 32, 1998.
- [16] A. Ebrahimpour and M. Maerefat, “A method for generation of typical meteorological year,” *Energy Conversion and Management*, vol. 51, no. 3, pp. 410–417, 2010.
- [17] A. L. Chan, T. Chow, S. K. Fong, and J. Z. Lin, “Generation of a typical meteorological year for hong kong,” *Energy Conversion and Management*, vol. 47, no. 1, pp. 87–96, 2006.
- [18] O. S. Ohunakin, M. S. Adaramola, O. M. Oyewola, and R. O. Fagbenle, “Generation of a typical meteorological year for north–east, nigeria,” *Applied Energy*, vol. 112, pp. 152–159, 2013.
- [19] S. Wilcox and W. Marion, “Users manual for tmy3 data sets (revised),” tech. rep., National Renewable Energy Lab.(NREL), Golden, CO (United States), 2008.
- [20] H. Hersbach, B. Bell, P. Berrisford, S. Hirahara, A. Horányi, J. Muñoz-Sabater, J. Nicolas, C. Peubey, R. Radu, D. Schepers, *et al.*, “The era5 global reanalysis,” *Quarterly journal of the royal meteorological society*, vol. 146, no. 730, pp. 1999–2049, 2020.
- [21] S. Sen and J. Roesler, “An uncoupled pavement-urban canyon model for heat islands,” in *Pavement Life-Cycle Assessment*, pp. 121–130, CRC Press, 2017.
- [22] A. M. Ioannides and L. Khazanovich, “Nonlinear temperature effects on multilayered concrete pavements,” *Journal of Transportation Engineering*, vol. 124, no. 2, pp. 128–136, 1998.

- [23] C. A. Donnelly, S. Sen, and J. M. Vandenbossche, “Reduction of critical positive temperature gradients in jointed plain concrete pavements,” *International Journal of Pavement Engineering*, vol. 24, no. 1, p. 2197645, 2023.
- [24] S. Sen, H. Li, and L. Khazanovich, “Effect of climate change and urban heat islands on the deterioration of concrete roads,” *Results in Engineering*, vol. 16, p. 100736, 2022.